

Electronic transport characterization of AlGaN/GaN heterostructures using quantitative mobility spectrum analysis

S. B. Lisesivdin, A. Yildiz, S. Acar, M. Kasap, S. Ozelik et al.

Citation: *Appl. Phys. Lett.* **91**, 102113 (2007); doi: 10.1063/1.2778453

View online: <http://dx.doi.org/10.1063/1.2778453>

View Table of Contents: <http://apl.aip.org/resource/1/APPLAB/v91/i10>

Published by the [American Institute of Physics](#).

Additional information on *Appl. Phys. Lett.*

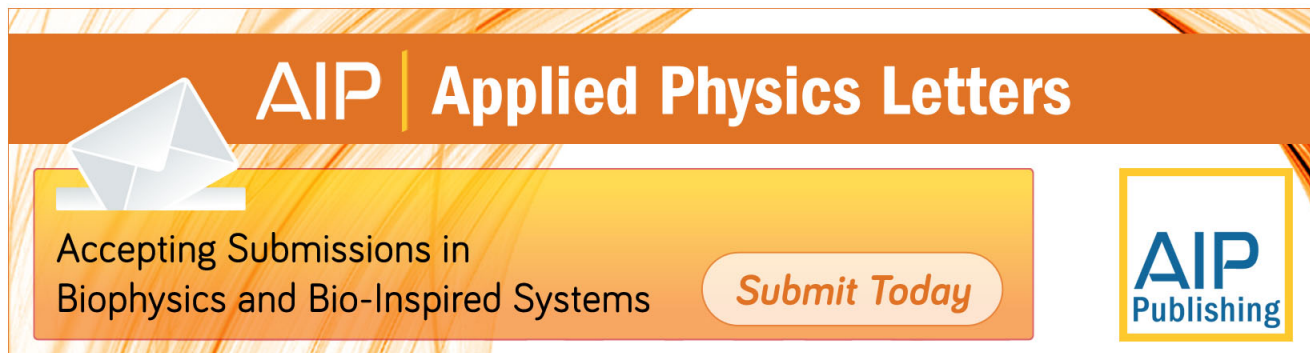
Journal Homepage: <http://apl.aip.org/>

Journal Information: http://apl.aip.org/about/about_the_journal

Top downloads: http://apl.aip.org/features/most_downloaded

Information for Authors: <http://apl.aip.org/authors>

ADVERTISEMENT



AIP | Applied Physics Letters

Accepting Submissions in
Biophysics and Bio-Inspired Systems

Submit Today

AIP
Publishing

Electronic transport characterization of AlGaN/GaN heterostructures using quantitative mobility spectrum analysis

S. B. Lisesivdin, A. Yildiz, S. Acar,^{a)} M. Kasap, and S. Ozelik

Department of Physics, Faculty of Science and Arts, University of Gazi, Teknikokullar, 06500 Ankara, Turkey

E. Ozbay

Nanotechnology Research Center, Department of Physics, and Department of Electrical and Electronics Engineering, Bilkent University, Ankara, Turkey

(Received 4 July 2007; accepted 9 August 2007; published online 6 September 2007)

Resistivity and Hall effect measurements in nominally undoped Al_{0.25}Ga_{0.75}N/GaN heterostructures grown on sapphire substrate by metal-organic chemical vapor deposition are carried out as a function of temperature (20–350 K) and magnetic field (0–1.5 T). The measurement results are analyzed using the quantitative mobility spectrum analysis techniques. It is found that there is strong two-dimensional electron gas localization below 100 K, while the thermally activated minority carriers with the activation energies of ~58 and ~218 meV contribute to the electron transport at high temperatures. © 2007 American Institute of Physics. [DOI: 10.1063/1.2778453]

High electron mobility transistors (HEMTs) are widely used and accepted as the promising components of the high-speed electronics. Especially, Al_xGa_{1-x}N/GaN HEMTs are the most interesting candidate since their introduction¹ and demonstration of high-power operability.² Due to their large band gap energy, large electron drift velocities, high conduction band discontinuity, and high thermal stability, Al_xGa_{1-x}N/GaN HEMTs can operate at high power and high temperature conditions with high two-dimensional electron gas (2DEG) sheet carrier density and high mobility values as compared even with GaAs based devices.^{3,4} Even without an intentional doping Al_xGa_{1-x}N/GaN interface, Al_xGa_{1-x}N/GaN based heterostructures have a 2DEG with high sheet carrier density values.^{5,6} The mobility and sheet carrier density of the 2DEG are the most important parameters in describing the electronic properties of Al_xGa_{1-x}N/GaN heterostructures. On the other hand, in practice, the charge carriers generated by the crystal defects in both bulk GaN and Al_xGa_{1-x}N layers, and the 2DEG carriers induced by the polarization at the interface can also contribute to the measured data and the electronic properties of Al_xGa_{1-x}N/GaN heterostructures. Therefore, even in nominally undoped Al_xGa_{1-x}N/GaN heterostructures, the mixed conduction can be presented.

However, in the presence of multiple carrier species, the mixed-conduction effects have a strong influence on electronic properties of semiconductor materials, including bulk samples, thin films, quantum wells, and multilayer device structures.⁷ Although single field Hall effect measurements extract only averaged mobility and carrier concentration, single field measurements are used to determine carrier concentration, band gap, and impurity activation energies and to describe the scattering process involved in the case of single electron, hole conduction, or single band conduction in the semiconductor. In the presence of mixed conduction, there is often a lack of an appreciation of the systematic errors when making these measurements and pitfalls in their interpretation and analysis since, in these measurements, it is assumed

that all carriers have the same drift velocity and the carrier mobility is identical to the minority carrier mobility.⁸ Therefore, in the mixed conduction case for extracting the correct transport parameters of the individual carriers, resistivity and Hall effect measurements are to be performed as a function of magnetic field. These measurements (variable field) allow us to simultaneously characterize densities and mobilities for each of the multiple electron and hole species. Several approaches for analyzing magnetic field dependent resistivity and Hall data from the samples exhibiting mixed conduction have been discussed in several papers.⁷⁻¹⁰

In this work, the variable field resistivity and Hall effect data were analyzed using the quantitative mobility spectrum analysis (QMSA) technique that described and improved in previous studies.¹¹⁻¹⁴ Variable field resistivity and Hall coefficient measurements in conjunction with the QMSA technique allow extraction of the individual carrier concentrations and mobilities in semiconductor materials. Thus, in this study, the individual carriers (2DEG and bulk carriers) and their effect on the electron transport are investigated using the QMSA technique in Al_{0.25}Ga_{0.75}N/GaN heterostructures grown by metal-organic chemical vapor deposition (MOCVD). In a number of papers, the QMSA technique has been used in determining individual carrier densities and mobilities in semiconductor materials, including bulk samples, thin films, quantum wells, and multilayer device structures.¹³⁻¹⁶

The samples investigated in this work were grown on *c*-plane (0001) sapphire (Al₂O₃) substrate in a low-pressure MOCVD reactor. The details of the samples are given elsewhere.¹⁷

For the resistivity and Hall effect measurements by the van der Pauw method, square shaped (5×5 mm²) samples were prepared with four evaporated Ti/Al/Ni/Au Ohmic contacts in the corners. The measurements were made at 24 temperature steps over a temperature range of 20–350 K using a Lake Shore Hall effect measurement system. At each temperature step, the Hall coefficient and resistivity were measured for both current directions, both magnetic field polarization, and all possible contact configurations at 31 magnetic field steps between 0 and 1.5 T. The magnetic field

^{a)} Author to whom correspondence should be addressed; FAX: 903122122279; electronic mail: sacar@gazi.edu.tr

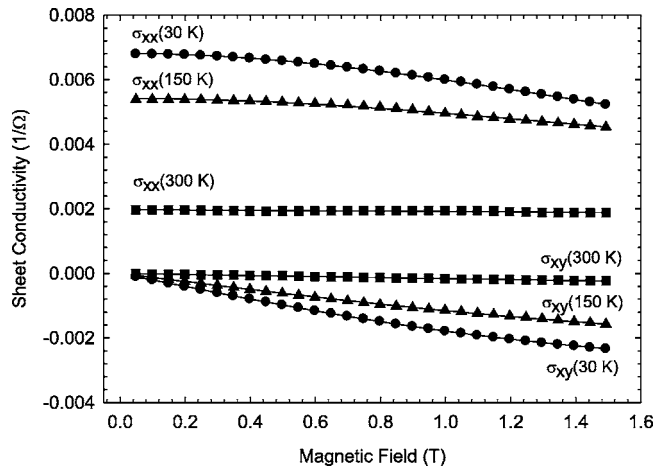


FIG. 1. Conductivity tensors vs magnetic field at 30, 150, and 300 K. The symbols are the experimental data. The lines represent the fits obtained from QMSA.

dependent data are analyzed using the QMSA technique. To confirm the activation energies obtained from the carrier densities, which extracted from QMSA, room temperature photoluminescence (RT-PL) measurements are also carried out with a Horiba Jobin-Yvon PL system with Kimmon 325 nm He–Cd laser.

To extract individual carriers from the measured field dependent data over studied temperature range are analyzed using the QMSA. First, the longitudinal and transverse conductivity tensors $\sigma_{xx}(B)$ and $\sigma_{xy}(B)$ at each temperature step are obtained using the field dependent resistivity and Hall coefficient data as the input parameters in QMSA. For the demonstration, the derived conductivity tensors (symbols) and the fitted results (solid lines) from QMSA are given in Fig. 1 for the only three temperatures. A near perfect fit (solid lines) to the data is a good indication of the validity of the QMSA spectrum presented below. It can also be seen from Fig. 1 that both the values of conductivity tensors, $\sigma_{xx}(B)$ and $\sigma_{xy}(B)$, increase with the decreasing temperature.

Second, we have performed the application of the QMSA technique to the measured field-dependent data to obtain the multicarrier mobility spectra at 24 temperature steps in the studied temperature range. For the demonstration, only the QMSA spectra at 30 and 195 K are given in Fig. 2. In the studied temperature range, some important distinct features of the mobility spectra have been observed. At

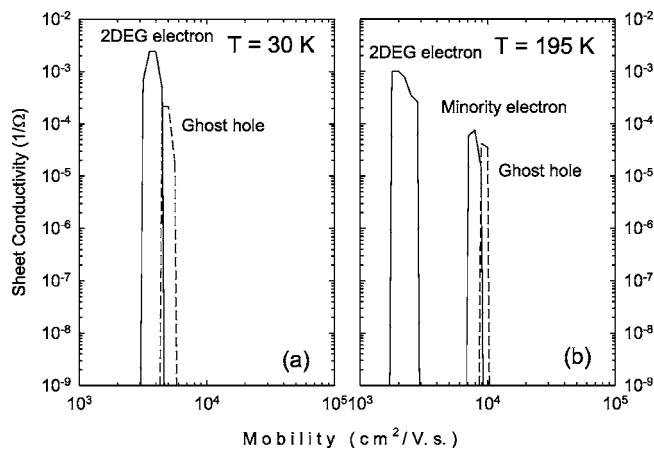


FIG. 2. Electron (solid lines) and hole (dashed lines) QMSA spectra for $\text{Al}_{0.25}\text{Ga}_{0.75}\text{N}/\text{GaN}$ heterostructure at (a) 30 and (b) 195 K.

whole temperature range, a main electron peak with a mobility close to the measured ones has been obtained from QMSA. At low temperatures (below 150 K), only one electron peak is observed, while at high temperatures two electron peaks are presented. In addition to these, at every temperature steps, hole peaks with a higher mobility than that of the last electron peak are observed. These peaks nearly overlap to the last electron peaks at the mobility spectrum, as can be seen from Fig. 2.

The mobility of the hole peaks is too high for any known carrier in the $\text{Al}_x\text{Ga}_{1-x}\text{N}/\text{GaN}$ heterostructures. For $\text{Al}_x\text{Ga}_{1-x}\text{N}/\text{GaN}$ material system, such an unexpected peak is, therefore, assumed to be unphysical and named as “ghost hole.” Such ghost holes are an artifact of a type that is seen quite frequently in mobility spectrum analyses and even in multicarrier fits.¹⁸ Several research groups have reported ghost carriers in their mobility spectrum analysis of different material systems and heterostructures, which emphasizes how pervasive such ghost carriers are.^{18,19} On the other hand, according to the layer structures,¹⁷ spontaneous and strain induced polarizations lead to a high positive polarization in the AlGaIn , resulting only in 2DEG induced at the $\text{Al}_x\text{Ga}_{1-x}\text{N}/\text{GaN}$ interface. In addition, our structure is undoped and it is well known that the crystal defects, such as Ga and N vacancies, in both GaN and AlGaIn layers produce shallow donor levels.²⁰ Therefore, in nominally undoped $\text{Al}_x\text{Ga}_{1-x}\text{N}/\text{GaN}$ heterostructures, only the negative charge carriers (2DEG and bulk electrons) are to be expected. To our knowledge, no satisfying explicit explanation for the actual mechanism of ghost carriers is reported yet. The possible origins of the ghost carriers may include nonideality of measurements and the assumptions made in the QMSA.

Figures 3(a) and 3(b) summarize the QMSA results as a function of temperature for the integrated density and mobility for each electron observed. In Figs. 3(a) and 3(b), the mobility and carrier density measured at 0.5 T are given with circles. From Fig. 3(b), it can be clearly understood that the polarizations induced 2DEG carrier species (n_1) and thermally activated carriers (n_2 and n_3) are obtained from QMSA. The mobility and electron density (triangles) for the 2DEG have the same temperature dependence with the measured mobility and carrier density at a single field (0.5 T), and their values are also closer to the measured ones. Both the measured (circles) and the 2DEG (triangles) mobility and carrier density are nearly independent of temperature below 100 K, where ionized impurity scattering would be expected to dominate. This behavior is typical of 2DEG structure. Above 100 K, Hall mobilities (measured and 2DEG) decrease with increasing temperature with a temperature dependence of $\sim T^{-3/2}$, which is the typical temperature dependence for phonon scattering mobility. The measured and 2DEG carrier densities still tend to be constant, which is a further confirmation of the 2DEG even at high temperature. Therefore, the analyses and measurement suggest that there is strong 2DEG localization below 100 K.

At high temperatures, the existed electrons with high mobility freeze out below 150 K. The existed minority carriers, which contribute much less to the total conductivity, have been assigned to bulk GaN. The remarkable point to note is that these carriers are quite distinctly evident at a density of only 10^{10} – 10^{12} cm^{-2} , despite the presence of the much more prominent 2DEG carrier species ($\sim 10^{13}$ cm^{-2}). Such sensitivity to low-density electrons has been observed

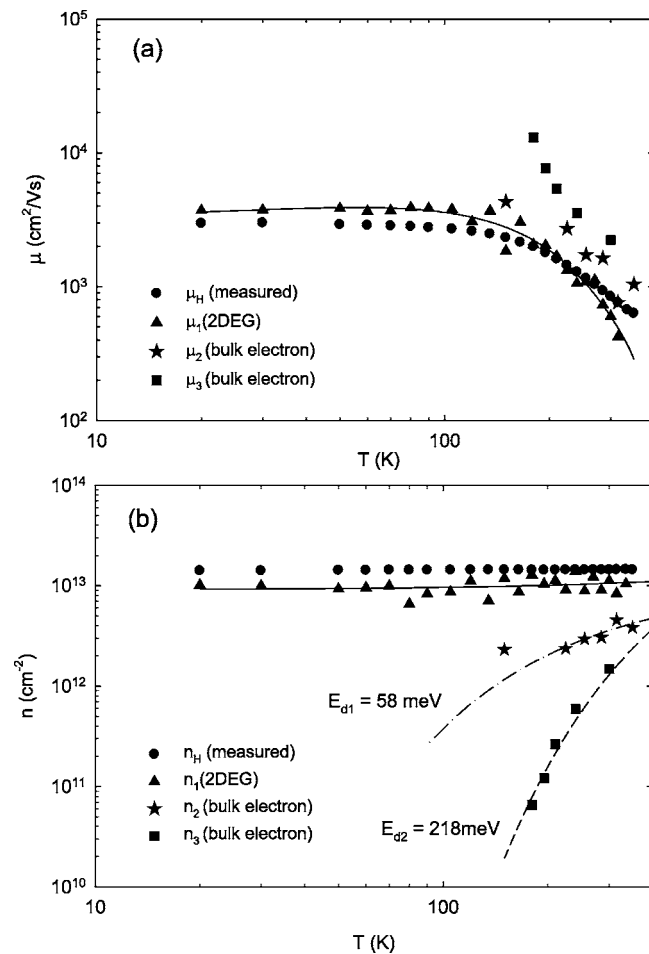


FIG. 3. (a) Mobility and (b) carrier concentration vs temperature. Circles represent measured mobility and carrier concentration at 0.5 T. Triangles, stars, and squares represent the mobilities and carrier concentrations extracted from QMSA. Solid lines shown are guides for the eye. Dash-dotted and dashed lines show the proposed trends of thermally activated minority carriers.

in the spectra for other semiconductor systems, and QMSA often yields more information about low-density minority carriers with high mobility than any of the other analysis techniques.¹² The activation energies of thermally generated minority carriers whose density increases exponentially with temperature are found to be ~ 58 and ~ 218 meV for n_2 and n_3 , respectively. We believe that these energies are related with the shallow defect (impurity and vacancy) levels of bulk GaN since the energies of shallow donor levels are reported ranging from 30 to 600 meV in GaN.²¹

To verify the activation energies obtained from the carrier densities given in Fig. 3(b), RT-PL measurements are also carried out. The results are analyzed using the multiple Gaussian peak analysis technique. RT-PL measurement and analysis results are shown in Fig. 4. Band gap energy (E_g) of GaN is obtained as ~ 3.41 eV. Three peaks are observed at 92.6, 56.1, and 223.4 meV below the conduction band edge. The energies of two peaks (56.1 and 223.4 meV) below E_C are close to the activation energies obtained from the extracted carriers from QMSA. Therefore, these two peaks are attributed as shallow defect levels in GaN. The other peak with 96.2 meV is evaluated as an optical phonon peak since such optical phonon related peaks are usually reported in literature.^{22,23} It is noted that the transition with 56.1 meV has more strength than the E_g transition due to overexcite-

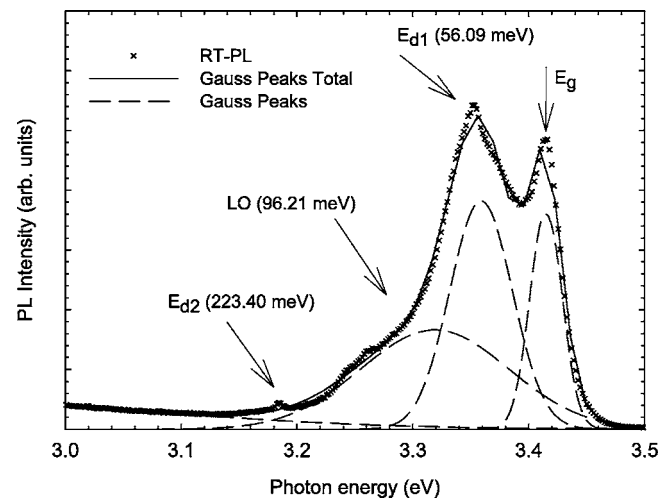


FIG. 4. Room temperature PL spectrum. Symbols represent PL measurements. Dashed and solid lines represent Gaussian peaks and total Gaussian peaks, respectively.

ment of the 3.81 eV laser, which is larger than the band gap energy.

- ¹M. A. Khan, A. Bhattarai, J. N. Kuznia, and D. T. Olson, *Appl. Phys. Lett.* **63**, 1214 (1993).
- ²Y. F. Wu, B. P. Keller, S. Keller, D. Kapolnek, P. Kozodoy, S. P. Denbaars, and U. K. Mishra, *IEEE Electron Device Lett.* **17**, 455 (1996).
- ³Y. F. Wu, B. P. Keller, P. Parikh, D. Kapolnek, S. P. Denbaars, and U. K. Mishra, *IEEE Electron Device Lett.* **18**, 290 (1997).
- ⁴R. Gaska, Q. Chen, J. Yang, A. Osinsky, M. A. Khan, and M. S. Shur, *IEEE Electron Device Lett.* **18**, 492 (1997).
- ⁵O. Ambacher, B. Foutz, J. Smart, J. R. Shealy, N. G. Weimann, K. Chu, M. Murphy, A. J. Sierakowski, W. J. Schaff, L. F. Eastman, R. Dimitrov, A. Mitchell, and M. Stutzman, *J. Appl. Phys.* **87**, 334 (2000).
- ⁶F. Bernardini, F. Fiorentini, and D. Vanderbilt, *Phys. Rev. B* **56**, R10024 (1997).
- ⁷J. R. Meyer, C. A. Hoffman, F. J. Bartoli, D. J. Arnold, S. Sivanathan, and J. P. Faurie, *Semicond. Sci. Technol.* **8**, 805 (1993).
- ⁸A. Wolkenberg, T. Przeslawski, J. Kaniewski, and K. Reginski, *J. Phys. Chem. Solids* **64**, 7 (2003).
- ⁹B. J. Kelley, B. C. Dodrill, J. R. Lindemuth, G. Du, and J. R. Meyer, *Solid State Technol.* **12**, 130 (2000).
- ¹⁰J. S. Kim, D. G. Seiler, and W. F. Tseng, *J. Appl. Phys.* **73**, 8324 (1993).
- ¹¹J. Antoszewski, D. J. Seymour, L. Farone, J. R. Meyer, and C. A. Hoffman, *J. Electron. Mater.* **24**, 1255 (1995).
- ¹²J. R. Meyer, C. A. Hoffman, J. Antoszewski, and L. Farone, *J. Appl. Phys.* **81**, 709 (1997).
- ¹³B. C. Dodrill, J. R. Lindemuth, B. J. Kelley, G. Du, and J. R. Meyer, *Compound Semicond.* **7**, 58 (2001).
- ¹⁴J. Antoszewski, L. Faraone, I. Vurgaftman, J. R. Meyer, and C. A. Hoffman, *J. Electron. Mater.* **33**, 673 (2004).
- ¹⁵M. Kasap and S. Acar, *Phys. Status Solidi A* **201**, 3113 (2004).
- ¹⁶S. Acar, M. Kasap, B. Y. Isik, S. Ozcelik, N. Tugluoglu, and S. Karadeniz, *Chin. Phys. Lett.* **22**, 2363 (2005).
- ¹⁷S. B. Lisesivdin, S. Acar, M. Kasap, S. Ozcelik, S. Gokden, and E. Ozbay, *Semicond. Sci. Technol.* **22**, 543 (2007).
- ¹⁸N. Biyikli, J. Xie, Y. T. Moon, F. Yun, C. G. Stefanita, S. Bandyopadhyav, H. Morkoç, I. Vurgaftman, and J. R. Meyer, *Appl. Phys. Lett.* **88**, 142106 (2006).
- ¹⁹N. N. Berchenko, V. V. Bogoboyashchii, I. I. Izhin, M. Pociask, E. M. Sheregii, and V. A. Yudenkov, *Phys. Status Solidi C* **2**, 1418 (2005).
- ²⁰Z. T. Zhou, L. W. Guo, Z. G. Xing, G. J. Ding, J. Zhang, M. Z. Peng, H. Q. Jia, H. Chen, and J. M. Zhou, *Chin. Phys. Lett.* **24**, 1641 (2007).
- ²¹V. Bougrov, M. E. Levinshtein, S. L. Rumyantsev, and A. Zubrilov, in *Properties of Advanced Semiconductor Materials GaN, AlN, InN, BN, SiC, SiGe*, edited by M. E. Levinshtein, S. L. Rumyantsev, and M. S. Shur (Wiley, New York, 2001), pp. 1–30.
- ²²H. S. Kwack, Y. H. Cho, G. H. Kim, M. R. Park, D. H. Youn, S. B. Bae, K. S. Lee, J. H. Lee, and J. H. Lee, *Phys. Status Solidi C* **6**, 2109 (2006).
- ²³S. M. Kim, H. S. Kwack, S. W. Hwang, Y. H. Cho, H. I. Cho, J. H. Lee, and K. L. Wang, *Phys. Status Solidi C* **6**, 2113 (2006).